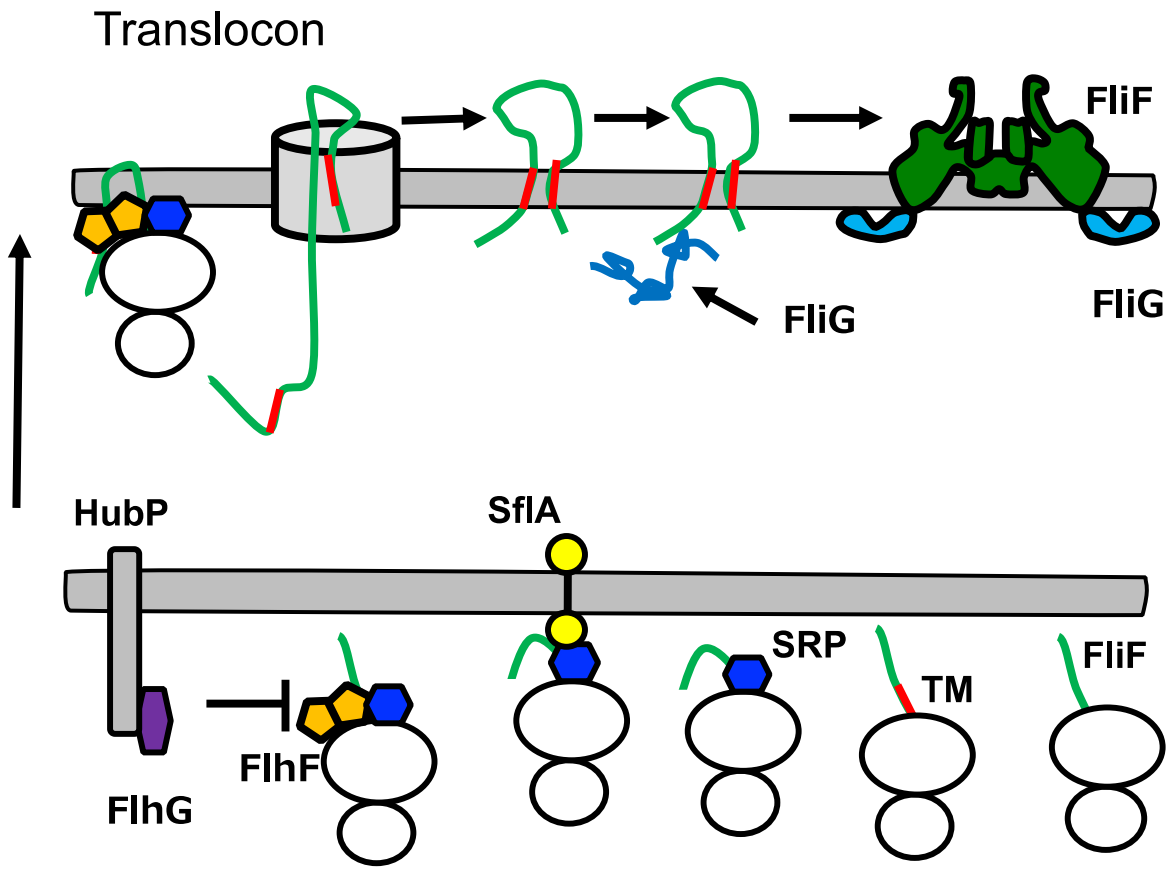

Supplementary Figure S1. A model of MS-ring formation made up of FliF proteins. SflA may interact with signal recognition particle (SRP) to prevent FliF from interacting with the SPR recognition particle. FlhF dominates the SflA protection process. FlhF may assist FliF in inserting the Sec translocon machinery. FliG supports the MS-ring formation by FliF.

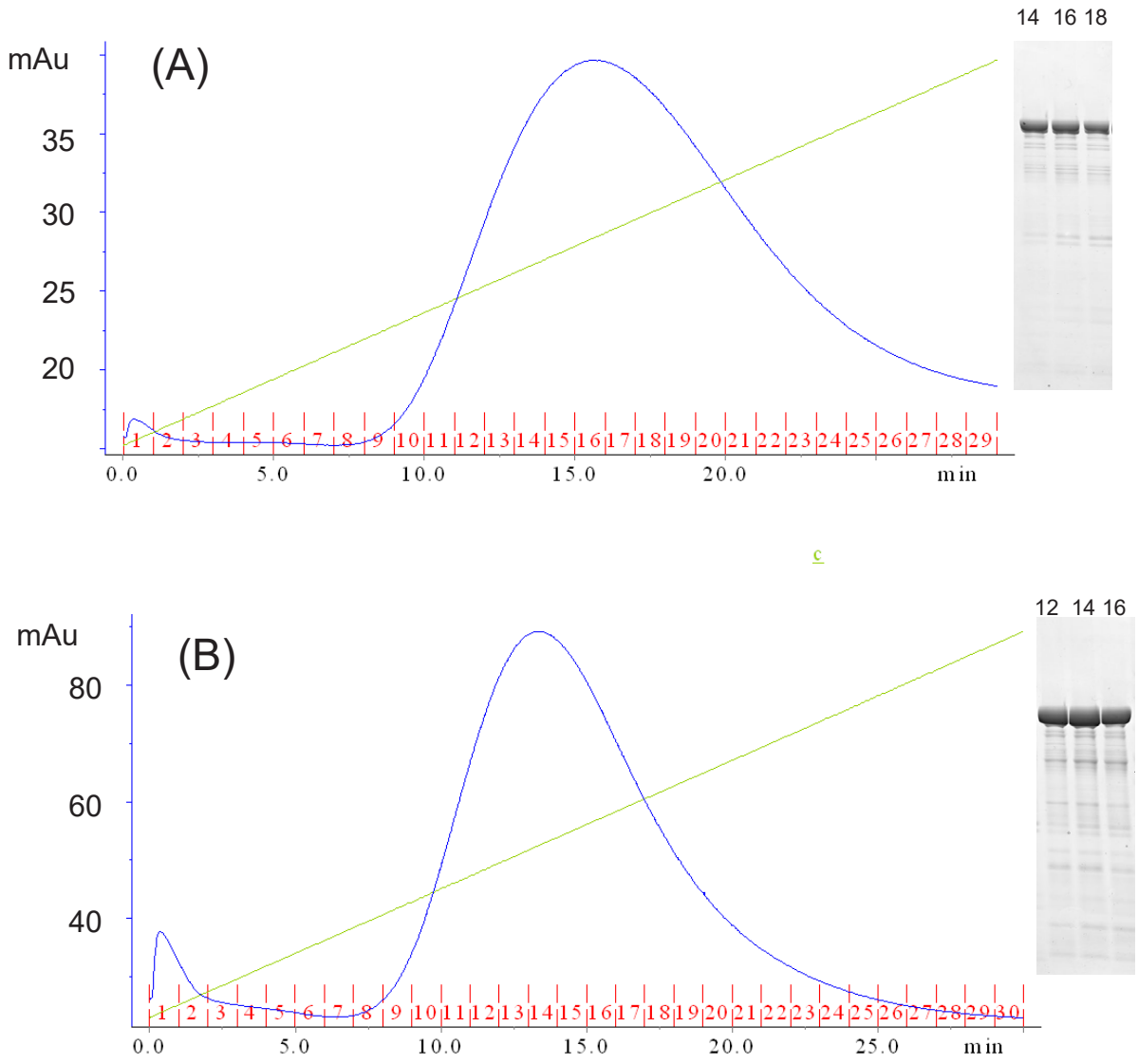

Supplementary Figure S2. His-tagged purification of MS-ring. The membrane lysate (A) or the soluble cytoplasmic lysate (B) solubilized in dodecyl maltoside (DDM) was loaded onto a 5 mL HiTrap TALON column washed with a buffer containing 10 mM imidazole, and the proteins were eluted with the linear gradient of 10 mM–300 mM imidazole. The proteins that were obtained in the fractions 14, 16, and 18 of (A) or the fractions 12, 14, 16 of (B) were separated using SDS-PAGE, stained with coomassie brilliant blue (CBB), and shown at the side of the elution profiles of (A) and (B).

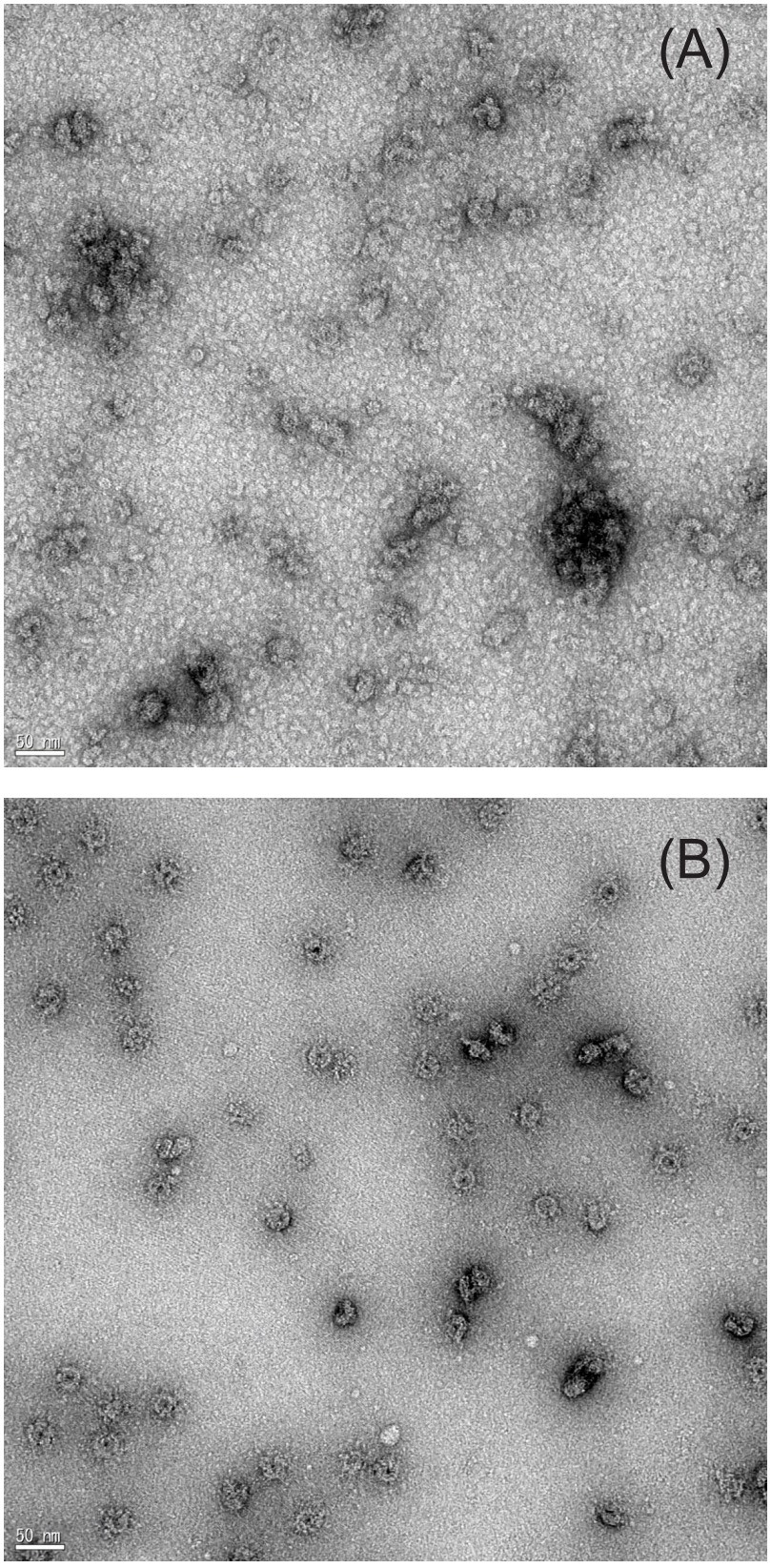

Supplementary Figure S3. Electron microscopic observation of MS-ring composed of FliFG fusion proteins. *E. coli* BL21 (DE3) cells housing pRO301 were cultured, and the MS-ring was isolated. The MS-ring was observed with an electron microscope in the membrane fraction (A) and the gel-filtration fraction (B). The scale bars; 50 nm.

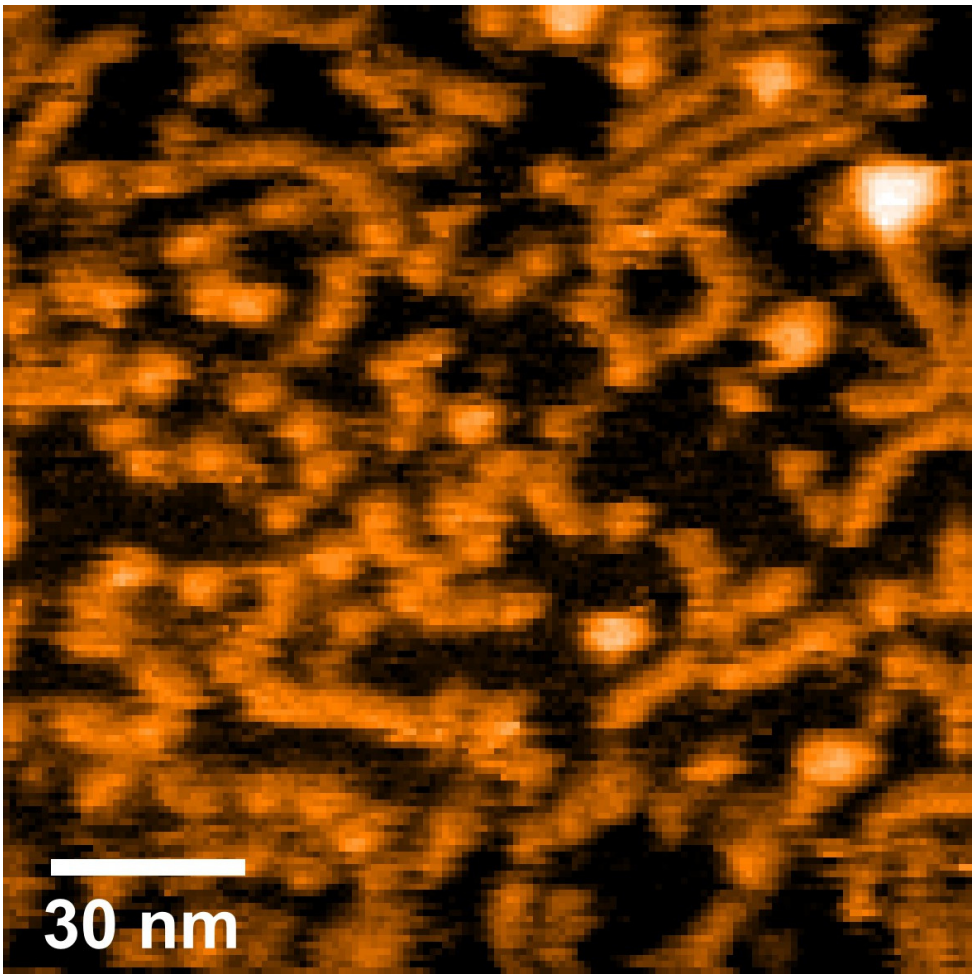

Supplementary Figure S4. AFM image of the (approximately) 350 kDa fraction. The peak fraction containing FliFG fusion protein at (approximately) 350 kDa using gel filtration and observed using HS-AFM.

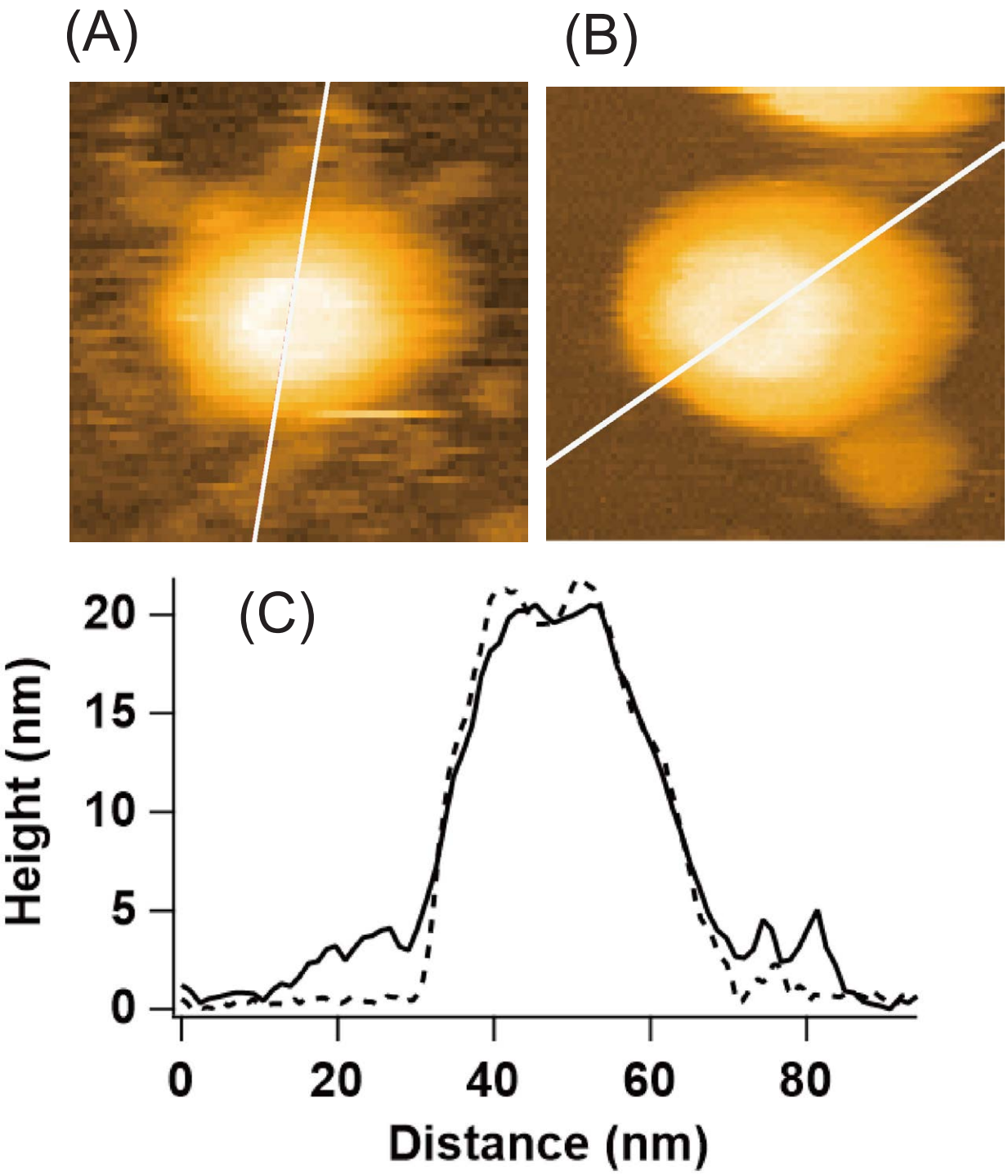

Supplementary Figure S5. HS-AFM image of MS-ring comprising FliFG fusion proteins (A) or FliF proteins (B). (C) The cross-sectional profiles of solid line and dotted line, along the white lines on the image of (A) and (B), respectively.

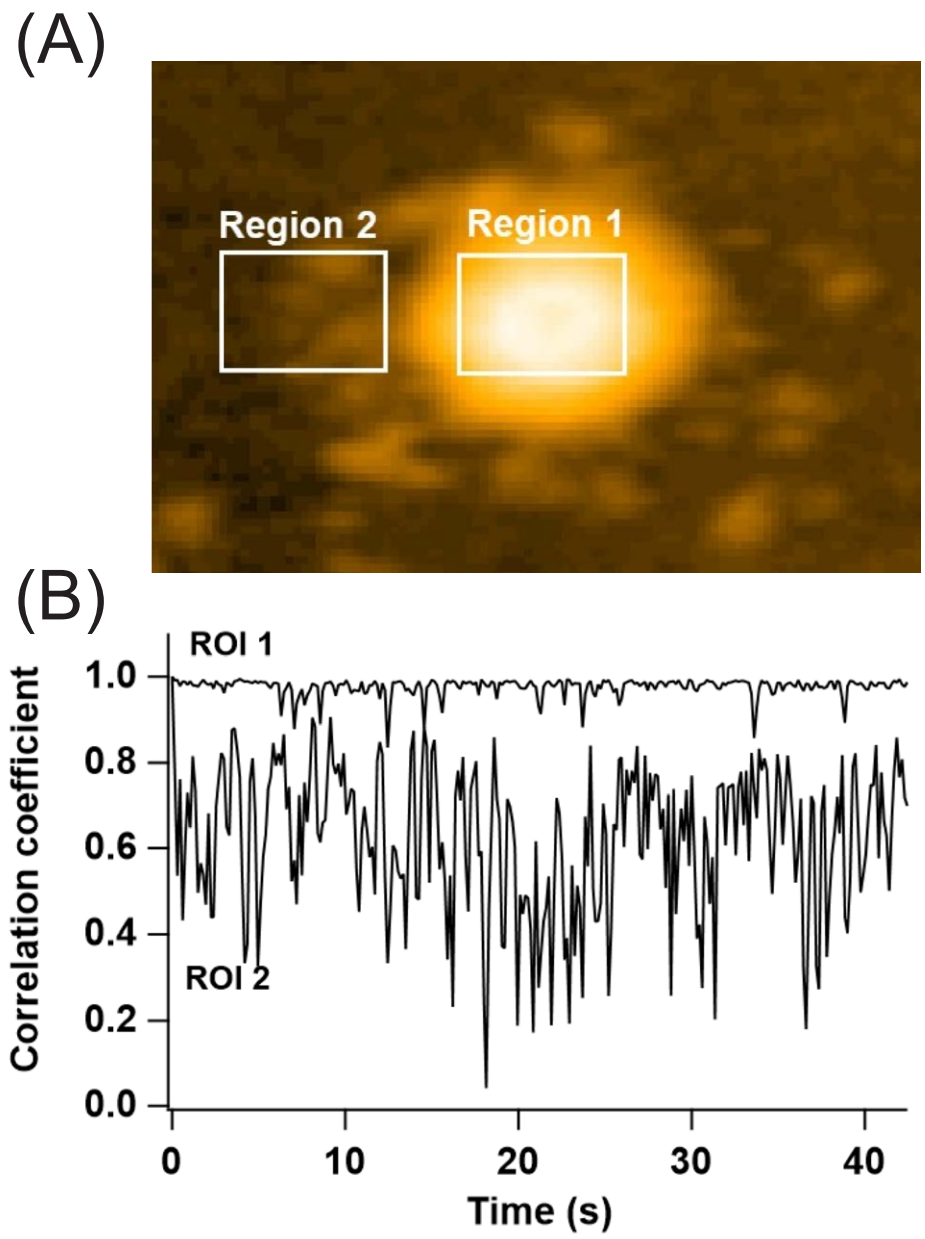

Supplementary Figure S6. (A) A image of MS-ring comprising FliFG fusion proteins by HS-AFM. (B) The correlation coefficients of ROI 1 and ROI 2 were plotted at the time of the image aquisition in the field of Region1 and Region2.

Supplementary Table S1. Bacterial strains and plasmids used in this study

Strain or plasmid	Genotype or description	Reference or source
E. coli		
DH5α	Recipient for DNA manipulation	
BL21(DE3)	expression host	Novagen
Plasmids		
pCold I	Amp^r, P_{cspA}	Takara
pRO101	pCold I-*his-fliF*	[1]
pTSK137	pCold I-*his-fliFG*	[2]
pRO301	pCold I-*his-fliFG* fusion	This study

Amp^r, ampicillin-resistant; Cm^r, chloramphenicol-resistant

[1] Ogawa, R., Abe-Yoshizumi, R., Kishi, T., Homma, M., Kojima, S. Interaction of the C-terminal tail of FliF with FliG from the Na^+-driven flagellar motor of *Vibrio alginolyticus*. J. Bacteriol. 197, 63-72 (2015). https://doi.org/10.1128/jb.02271-14

[2] Terashima, H., Hirano, K., Inoue, Y., Tokano, T., Kawamoto, A., Kato, T., et al. Assembly mechanism of a supramolecular MS-ring complex to initiate bacterial flagellar biogenesis in *Vibrio* species. J. Bacteriol. 202, e00236-20 (2020). https://doi.org/10.1128/jb.00236-20

Supplementary Movie S1. High-speed atomic force microscopy (HS-AFM) movies of MS-ring composed of FliFG fusion proteins. Real-time play speed: 0.15 s/frame.